nature communications

Article

https://doi.org/10.1038/s41467-023-41364-w

CD8$^+$ tissue-resident memory T-cell development depends on infection-matching regulatory T-cell types

Received: 17 September 2022

Accepted: 29 August 2023

Published online: 11 September 2023

Check for updates

Leandro Barros[1], Daryna Piontkivska[2], Patrícia Figueiredo-Campos[1], Júlia Fanczal[1], Sofia Pereira Ribeiro[1], Marta Baptista[1], Silvia Ariotti[1], Nuno Santos[3,5], Maria João Amorim[3,4], Cristina Silva Pereira[2], Marc Veldhoen[1,6] ✉ & Cristina Ferreira[1,6] ✉

Immunological memory is critical for immune protection, particularly at epithelial sites, which are under constant risk of pathogen invasions. To counter invading pathogens, CD8$^+$ memory T cells develop at the location of infection: tissue-resident memory T cells (T_{RM}). CD8$^+$ T-cell responses are associated with type-1 infections and type-1 regulatory T cells (T_{REG}) are important for CD8$^+$ T-cell development, however, if CD8$^+$ T_{RM} cells develop under other infection types and require immune type-specific T_{REG} cells is unknown. We used three distinct lung infection models, to show that type-2 helminth infection does not establish CD8$^+$ T_{RM} cells. Intracellular (type-1) and extracellular (type-3) infections do and rely on the recruitment of response type-matching T_{REG} population contributing transforming growth factor-β. Nevertheless, type-1 T_{REG} cells remain the most important population for T_{RM} cell development. Once established, T_{RM} cells maintain their immune type profile. These results may have implications in the development of vaccines inducing CD8$^+$ T_{RM} cells.

Epithelial barriers are prime portals for microbial invasion. Organ structure, such as a multilayer of epithelial cells in the skin, provides additional protection against invasion. Other organs, such as the intestine and lung require optimal exchange of nutrients, liquids, and gasses that necessitate a single epithelial cell layer. It is highly beneficial to the host to contain invading pathogens at the site of entry and swiftly clear any pathogens and their products to avoid tissue damage and systemic dissemination of infectious or toxic material. For this reason, the immune response is tailored to the identity of the invading microbe, towards intracellular (type-1), helminths (type-2), or extracellular (type-3) pathogens. Understanding how tissue immunity is established following distinct responses has conceivable therapeutic potential with the ability to modulate tissue-specific immunity, from vaccination strategies to tumour treatment.

The development of immunological memory is a pillar of adaptive immunity and an efficacious way to prevent the development of disease caused by pathogen entry. Memory T lymphocytes are functionally and phenotypically classified in at least three subsets. Central memory (T_{CM}) and effector memory (T_{EM}) T cells recirculate throughout lymphoid and non-lymphoid organs respectively[1]. T_{EM} cells actively scout for pathogens, entering and exiting organs via the circulation and lymph, while T_{CM} cells are more quiescent and are reactivated in secondary lymphoid organs, faster than, but not dissimilarly from, naïve T cells[2,3]. Although these cells provide significant

[1]Instituto de Medicina Molecular | João Lobo Antunes, Faculdade de Medicina da Universidade de Lisboa, Av. Professor Egas Moniz, Lisbon 1649-028, Portugal. [2]Instituto de Tecnologia Química e Biológica António Xavier, Av. da República, Oeiras 2780-157, Portugal. [3]Instituto Gulbenkian de Ciência, Rua da Quinta Grande 6, Oeiras 2780-156, Portugal. [4]Universidade Católica Portuguesa, Católica Médical School, Católica Biomedical Research Centre, Palma de Cima 1649-023, Portugal. [5]Present address: The Francis Crick Institute, 1 Midland Road, London NW1 1AT, UK. [6]These authors contributed equally: Marc Veldhoen, Cristina Ferreira. ✉e-mail: marc.veldhoen@medicina.ulisboa.pt; cristina.ferreira@medicina.ulisboa.pt

protection from recurrent infections due to increased antigen-specific numbers and speed of activation, they require a systemic immune reaction for triggering and may not be sufficiently efficacious against pathogen entry. Tissue-resident memory (T_{RM}) T cells reside in tissues, especially those at the host/environment interface. T_{RM} cells actively survey the tissues for signs of infection, able to react rapidly and thereby swiftly eliminate infected cells without the need for a systemic immune reaction[1].

$CD8^+$ T_{RM} cells are characterised by the expression of different markers and transcription factors, which depend on their activation status and on the tissue type they home to[4]. Most T_{RM} cells constitutively express CD69, which antagonises the egress receptor S1P receptor 1, thus maintaining tissue residency[5–7], with organ specificity[8]. The integrins CD103 and CD49a are additional markers of tissue residency, although T_{RM} cells negative for CD103 have been reported and CD49a may reflect activation status[9–12]. CD103, integrin αE pairing with β7, is mostly present on epithelial residing T_{RM} cells, providing support for tissue homing and maintenance via epithelial cell E-cadherin binding, while potentiating cytolytic activity. Of additional importance is the absence of Killer Cell Lectin Like Receptor G1 (KLRG1), typically described as a terminal differentiation marker on effector T cells[13,14]. KLRG1 may compete with CD103 for the binding to E-cadherin, with its downregulation contributing to T_{RM} cell residency[15].

A transcriptional programme, distinct from other $CD8^+$ T-cell subsets, drives surface markers and function of T_{RM} cells. T_{RM} cells express low levels of Tbox protein expressed in T cells (Tbet) and Krüppel-like Factor 2 (KLF2), while Eomesodermin (Eomes) is absent[6,14,16]. Instead, T_{RM} cells express high levels of arylhydrocarbon receptor (AhR) in gut and skin, Hobit and Blimp-1[17,18]. In addition, T_{RM} cells are maintained in a semi-activation state and distinct metabolic wiring takes place, ensuring rapid full activation when required[19,20].Thus, T_{RM} cells patrol non-lymphoid organs and perform immunosurveillance by killing infected cells and producing cytokines to recruit other immune cells to quickly eliminate the pathogen[21,22].

Exacerbated T-cell responses can result in tissue damage, and a balance between pathogen elimination and immunopathology needs to be maintained. Regulatory T cells (T_{REG}), characterised by the expression of Forkhead box protein 3 (Foxp3) transcription factor, play an important role in reducing excessive immune responses. T_{REG} can influence the transition of effector $CD8^+$ T cells to memory cells by limiting interleukin (Il)−2 availability, producing Il-10 and cytotoxic T-lymphocyte associate protein-4 (CTLA-4)[23–25]. Of importance, T_{REG} cells can adopt a transcriptional programme in line with the type of inflammation and the $CD4^+$ T helper (T_H) subset involved. Besides Foxp3, T_{REG} cells can co-express the T_H1 cell (type-1) factor Tbet, the T_H2 cell (type-2) factor Gata-3, and the T_H17 cell (type-3) factor Rorγt, to take on characteristics of one of these T_H cell ineages[22,26–28].

We previously showed that type-1 T_{REG} cells, recruited via their Tbet-dependent expression of the chemokine receptor CXCR3, supply and activate transforming growth factor (TGF)β locally, thereby efficiently facilitating the generation of T_{RM} cells[14]. However, although T_{RM} cells were found reduced in several organs, the link between their generation and type-1 T_{REG} cells was established in the intestine and during a type-1 immune response. This raises the question of whether the establishment of T_{RM} cells in another organ is also dependent on type-1 T_{REG} cells, and more importantly, whether T_{RM} cell development during other types of infection is dependent on the corresponding type of T_{REG} cell or remains dependent on type-1 T_{REG} cells. Here, we show that, in the lung, type-1 T_{REG} cells are required to establish T_{RM} cells upon type-1 infection, while a type-2 infection does not establish a robust T_{RM} cell population. Furthermore, type-3 infection in the same organ requires type-3 T_{REG} cells and their provision of TGFβ for efficient T_{RM} cell establishment.

Results

Type-1 immunity induces T_{RM} cells in lungs

In the absence of type-1 T_{REG}, there is a reduction in $CD8^+$ T_{RM} cells in the intestine, lungs, and liver, due to inhibition of their generation[14]. To establish a robust infection model in the lungs, we infected $Foxp3^{WT}$ mice with influenza H3N2 (X-31). A week after influenza infection, a robust influx of $CD4^+$ and $CD8^+$ T cells is observed (Supplementary Fig. 1a–d). Influenza challenge results in a strongly polarised type-1 response with production of interferon (IFN)-γ and dominance of CXCR3-expressing $CD4^+$ and $CD8^+$ T cells, with no other polarised T-cell response observed (Fig. 1a–d; Supplementary Fig. 1e–h). In addition to the type-1 response of $CD4^+$ and $CD8^+$ T cells, predominantly type-1 T_{REG} cells expressing CXCR3 (Fig. 1e–f) are recruited to the site of inflammation.

Influenza infection results in the establishment of a substantial $CD8^+$ T_{RM} cell population (Fig. 1g–h). To understand if their establishment in the lungs upon influenza infection is dependent on type-1 T_{REG} cells we make use of our previously setup transfer model whereby CD45.1 expressing $CD8^+$ T cells ($CD8^{CD45.1}$) are transferred into control $Foxp3^{Wt}$ mice or $Foxp3^{\Delta Tbx21}$ mice that miss type-1 T_{REG}[14]. Cells are readily recovered in the spleens, and the characteristic weight loss is observed (Supplementary Fig. 1i–k). As previously shown in the small intestine, the absence of type-1 T_{REG} cells reduces the establishment of $CD8^+$ T_{RM} cells, after $CD8^{CD45.1}$ transfer. We now extend this observation to the lungs upon influenza infection where compared to controls ($Foxp3^{WT}$), the absence of type-1 T_{REG} cells leads to reduced efficiency of $CD8^+$ T_{RM} cell development (Fig. 1i).

Type-2 immunity does not induce de novo $CD8^+$ T_{RM} cells in lungs

Establishment of $CD8^+$ T_{RM} cells in the lung with similar requirements to the small intestine may still rely on the type-1 inflammation induced by an intracellular pathogen as influenza virus. We subsequently used the helminth *Nippostrongylus brasiliensis*, widely used as a model to elicit strong type-2 immunity in the lungs[29]. A week after infection we observe a strong activation of $CD4^+$ T cells, $CD44^{hi}$, and a response characterised by T_H2 cells in the lungs expressing IL-4 and IL-13 (Fig. 2a, b; Supplementary Fig. 2a, b)[30]. However, the $CD8^+$ T-cell compartment shows a very limited effector $CD44^{hi}$ $CD8^+$ T-cell response, without type-2 polarisation, with primarily IFN-γ produced (Fig. 2c, d). There is an influx of T_{REG} cells, but without a polarisation towards any specific T_{REG} subset (Fig. 2e, f). Although some endogenous $CD8^+$ T_{RM} cell accumulation is observed, the CD8 T-cell activation in the lungs is modest (Fig. 2g, h, Supplementary Fig. 2c, d).

$CD8^{CD45.1}$ and $CD4^{CD45.1}$ T cells transferred into $Foxp3^{Wt}$ mice are recovered from the spleen, with robust numbers but without signs of activation with the majority of cells showing a naïve or T_{CM} cell phenotype (Supplementary Fig. 2e–g). $CD8^{CD45.1}$ T cells are few in the lungs upon infection, with $CD8^+$ T_{RM} cells rare and often below the detection threshold (Fig. 2i–l). $CD4^{CD45.1}$ T cells are more numerous in the lungs upon infection, at cost of cell numbers in the spleen, with $CD4^+$ T_{RM} cell proportions much higher than $CD8^+$ T_{RM} cells (Supplementary Fig. 2g–h). This indicated robust $CD4^+$ T-cell recruitment to the site of *N. brasiliensis* infection as opposed to $CD8^+$ T cells. Comparing influenza and *N. brasiliensis*, $CD8^{CD45.1}$ T cells remain abundant upon type-2 infection in the spleen, while transferred $CD8^+$ T cells are recruited to the site of infection only after challenge with influenza (Fig. 2m, n). Although $CD8^+$ T_{RM} cell generation is efficient in lung tissue, with $CD8^+$ T cells recruited and relying on type-1 T_{REG} cell help during a type-1 immune response, a type-2 infection, despite a robust $CD4^+$ T-cell response (Fig. 2a, b), does not result in de novo $CD8^+$ T-cell recruitment, activation or polarisation, the recruitment of type-2 T_{REG} cells, or the establishment of $CD8^+$ T_{RM} cells.

https://doi.org/10.1038/s41467-023-41364-w

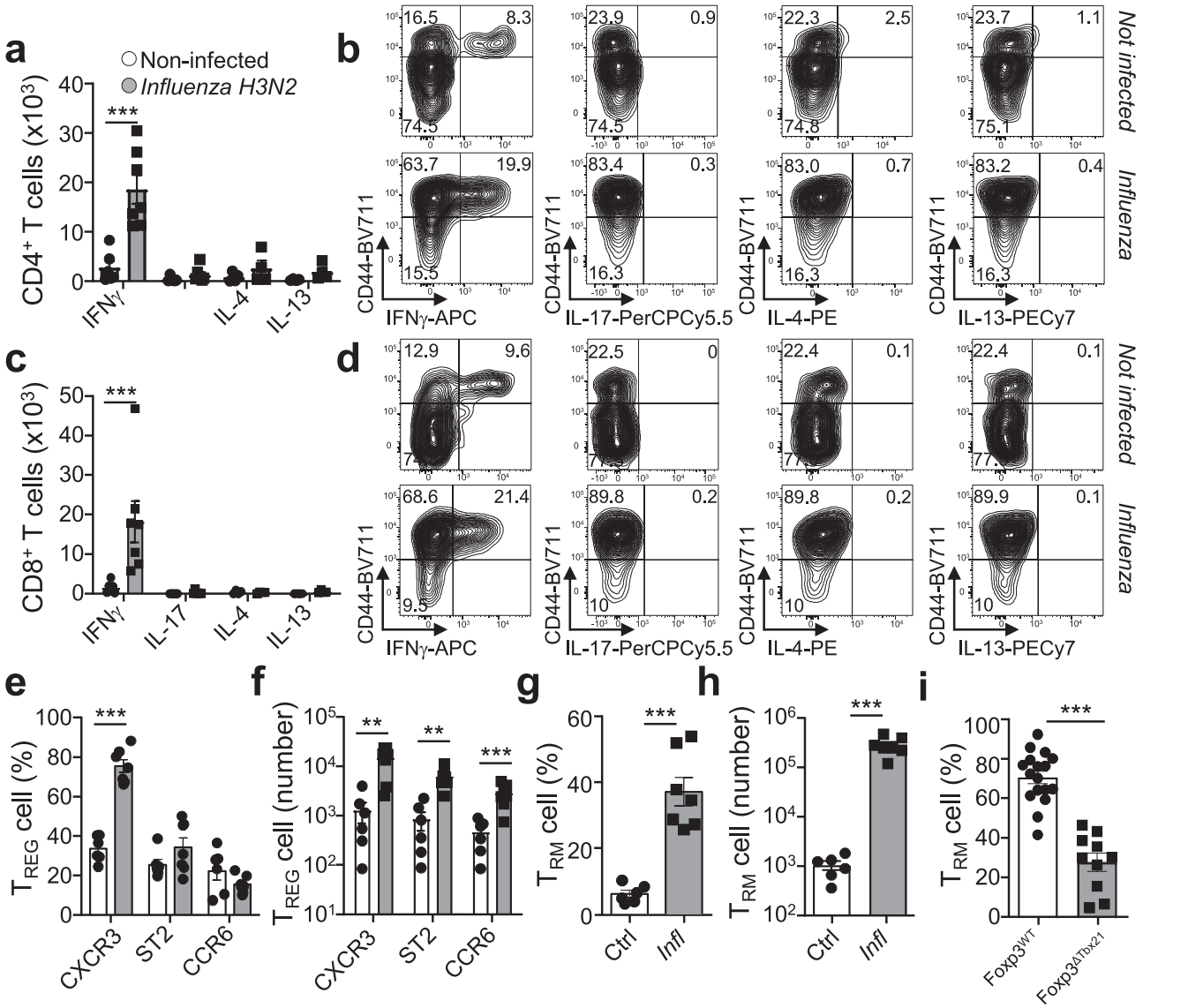

Fig. 1 | Type-1 TREG cells are required for TRM cell generation in the lungs upon Influenza infection. Mice were infected or not intranasally with 1000 plaque-forming units (PFU) of Influenza A X-31 strain (H3N2). 10 days post-infection lungs were collected, and cells were isolated and analysed via flow cytometry for cytokine production. **a** Numbers of activated ($CD44^+$) $CD4^+$ T cells producing indicated cytokines ($p_{(\text{Non-infected vs. Influenza H3N2})} < 0.000001$) and (**b**) representative flow cytometry plots ($n = 6$, non-infected, $n = 7$ infected, $N = 3$). **c** Numbers of activated $CD8^+$ T cells producing indicated cytokines ($p_{(\text{Non-infected vs. Influenza H3N2})} = 0.000013$) and **d** representative flow cytometry plots ($n = 6$, non-infected, $n = 7$ infected, $N = 3$). **e**, **f** $Foxp3^{WT}$ mice ($n = 6$, non-infected, $n = 7$ infected, $N = 3$) were assessed for **e** percentage ($p_{(\text{Non-infected vs. Influenza H3N2})} < 0.000001$), and **f** numbers of chemokine receptors CXCR3, ST2 (IL-33R) and CCR6 expression ($p_{(\text{Non-infected vs Influenza H3N2})}$: CXCR3, $p = 001415$; ST2, $p = 0.000502$; CCR6, $p = 0.001132$), on T_{REG} cells ($n = 6$, non-infected, $n = 8$ infected, $N = 3$). **g**, **h** Mice analysed via flow cytometry for **g** percentages of total $CD8^+$ T cells and **h** numbers of T_{RM} cells, defined as $CD69^+KLRG1^-$ $CD8^+$ T cells, $p_{(\text{Non infected vs Influenza H3N2})} < 0.0001$ ($n = 6$, $N = 3$). **i** $Foxp3^{WT}$ and $Foxp3^{\Delta Tbx21}$ mice received $CD8^{CD45.1}$ T cells intravenously, one day prior to infection. 14 days post infection, lung cells were assessed by flow cytometry for the percentage of T_{RM} cells ($CD69^+KLRG1^-CD103+$) in the transferred population ($Foxp3^{WT}$ $n = 17$, $Foxp3^{\Delta Tbx21}$ $n = 10$, $N = 4$), $p_{(\text{Foxp3WT vs Foxp3}\Delta\text{Tbx21})} < 0.0001$. Two-sided Mann–Whitney analysis was applied to compare groups. Data are presented as bars of mean ± SEM with single data points.

Type-3 immunity does induce $CD8^+$ T_{RM} cells in lungs

Besides intracellular pathogens resulting in robust $CD8^+$ T_{RM} cell development, we asked if extracellular pathogens, not helminths, would result in the generation of $CD8^+$ T_{RM} cells. *Aspergillus fumigatus* infection results in a robust response dominated by T_H17 cells (Fig. 3a, b; Supplementary Fig. 3a, b)[31]. In contrast to a type-2 infection, a type-3 challenge shows a type-1 response with increased numbers of T_H1 accompanied by a robust $CD44^{hi}$ effector $CD8^+$ T-cell response, but with few expressing IFN-γ, yet IL-17 production is observed (Fig. 3c, d; Supplementary Fig. 3c, d).

The influx of T_{REG} cells shows skewing towards type-3 T_{REG} at cost of type-1 T_{REG} cells, with total T_{REG} cell numbers increasing for all subsets (Fig. 3e, f). The T_{REG} cell response reflects the $CD4^+$ T-cell response, which shows strong skewing towards $Ror\gamma t^+CCR6^+$ T_H17 cells, but with increased numbers in all subsets (Supplementary Fig. 3e–g). The proportional distribution of $CD8^+$ T cells remains similar to uninfected, but with total numbers of type-3 $CD8^+$ T cells increasing (Supplementary Fig. 3h–j). *Aspergillus* infection increases endogenous host $CD8^+$ T_{RM} cell numbers in the lungs (Fig. 3g, h). Upon adoptive transfer of $CD8^{CD45.1}$ T cells, in contrast to the type-2 infection used, newly established $CD8^+$ T_{RM} cells were more robustly detected upon *Aspergillus* challenge compared to *N. brasiliensis* infection (Fig. 3i). In summary, type-1 and 3 infections result in $CD8^+$ T_{RM} cell formation, which is not observed for a type-2 immune response.

https://doi.org/10.1038/s41467-023-41364-w

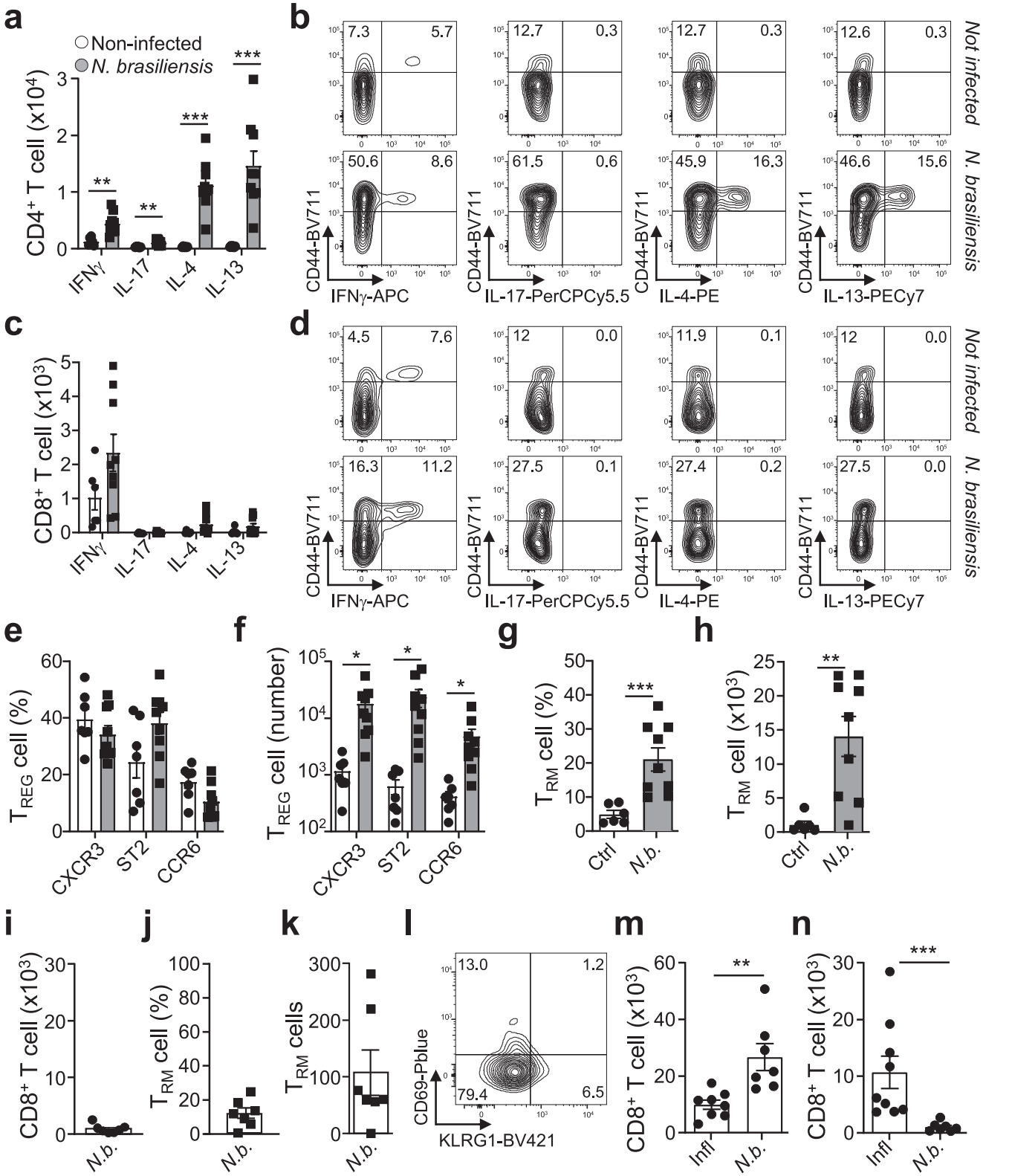

Deletion of Rorγt in FoxP3$^+$ cells ablates type-3 T_{REG} cells

Our results using the type-3 immunity-inducing fungi *Aspergillus* indicate that CD8$^+$ T_{RM} cells are induced during type-3 infections. This raises the question if T_{REG} cells are required and if the type of T_{REG} cell needs to match the infection type to efficiently establish CD8$^+$ T_{RM} cells after type-3 infections. In order to address this, we generated Foxp3-yfp-Cre Rorγt$^{f/f}$ mice (Foxp3$^{\Delta Ror\gamma t}$), in which type-3 T_{REG} cells are efficiently removed similarly as to type-1 T_{REG} cells in Foxp3$^{\Delta Tbx21}$ mice, in all tissues assayed (Fig. 4a, b)[14]. CD4$^+$ or CD8$^+$ T-cell proportions or numbers, including Rorγt-expressing subsets such as T_H17 cells, or T_{REG} subset proportions and numbers are not altered in Foxp3$^{\Delta Ror\gamma t}$ mice compared to controls (Fig. 4b–d; Supplementary Fig. 4a–d). Since type-1 T_{REG} cells are important in CD8$^+$ T_{RM} cell formation[14], we also determined proportion and numbers of type-1 T_{REG} cells and CXCR3 expression. These are similar between Foxp3^{Wt} and Foxp3$^{\Delta Ror\gamma t}$ mice (Fig. 4b, e, f; Supplementary Fig. 4c, e). In agreement with the

Fig. 2 | Type-2 Nippostrongylus brasiliensis infection does not yield CD8 TRM cell formation. Mice were subcutaneously infected or not with 300 stage L3 larvae of *Nippostrongylus brasiliensis*. 7 days post-infection lungs were collected, and cells were isolated and analysed via flow cytometry for cytokine production, and T_{RM} cells. **a** Numbers of activated ($CD44^+$) $CD4^+$ T cells producing indicated cytokines, $p_{(\text{Non-infected vs } \textit{Nippostrongylus brasiliensis})}$: IFN-γ, $p = 0.001749$; IL-17, $p = 0.002537$; IL-4, $p = 0.000048$; IL-13, $p = 0.000729$, and **b** representative flow cytometry plots (non-infected $n = 6$, infected $n = 9$, $N = 3$). **c** Numbers of activated $CD8^+$ T cells producing indicated cytokines and **d** Representative flow cytometry plots of cytokine production in $CD8^+$ T cells (non-infected $n = 6$, infected $n = 9$, $N = 3$). **e**, **f** $Foxp3^{WT}$ mice were assessed for **e** percentage and **f** numbers of chemokine receptors CXCR3, ST2 (IL-33R) and CCR6 expression on T_{REG} cells, $p_{(\text{Non-infected vs } \textit{Nippostrongylus brasiliensis})}$: CXCR3, $p = 0.014118$; ST2, $p = 0.023778$; CCR6, $p = 0.028885$, (non-infected $n = 6$, infected $n = 9$, $N = 3$). **g**, **h** $CD69^+KLRG1^-$ $CD8^+$ T_{RM} cell **g** percentage of total $CD8^+$ T cells, $p_{(\text{Non-infected vs } \textit{Nippostrongylus brasiliensis})} = 0.0004$, and **h** number, $p_{(\text{Non-infected vs } \textit{Nippostrongylus brasiliensis})} = = 0.0016$, in non-infected (control) and infected mice (non-infected $n = 6$, infected $n = 9$, $N = 3$). **i**–**l** $Foxp3^{WT}$ mice received $CD8^{CD45.1}$ T cells intravenously, one day prior to infection. 14 days post-infection, lung cells were analysed via flow cytometry for **i** total number of $CD8^{CD45.1}$ T cells, $CD69^+KLRG1^-$ $CD8^+$ T_{RM} cell **j** percentage and **k** numbers, and **l** representative flow plot, within the $CD8^{CD45.1}$ T-cell population ($n = 7$, $N = 3$). **m**, **n** Comparison of transferred $CD8^{CD45.1}$ T-cell number in the (**m**) spleen, $p_{(\text{Influenza vs } \textit{Nippostrongylus brasiliensis})} = 0.0012$, or (**n**) lungs, $p_{(\text{Influenza vs } \textit{Nippostrongylus brasiliensis})} = 0.0002$, of mice infected with *Influenza* and *N. brasiliensis* (*Influenza* $n = 9$, *N. brasiliensis* $n = 7$, $N = 3$). 2-sided Mann–Whitney analysis was applied to compare the differences between groups. Data is presented as bars of mean ± SEM with single data points.

presence of similar numbers of type-1 T_{REG} cells, the number of intraepithelial lymphocytes (IELs) and $CD8^+$ T_{RM} cells in the lamina propria lymphocytes (LPL), lung, and liver, which differ in $Foxp3^{\Delta Tbx21}$ mice[14], were comparable between $Foxp3^{Wt}$ and $Foxp3^{\Delta Roryt}$ mice (Fig. 4g; Supplementary Fig. 4f–h). Collectively, the data shows that efficient deletion of type-3 T_{REG} cells is established without effects on other T-cell populations, as well as a noticeable effect on $CD8^+$ T_{RM} cells present at steady state.

Deletion of type-3 T_{REG} cells impacts $CD8^+$ T_{RM} cell formation

Segmented filamentous bacteria (SFB) are known inducers of T_H17 cells[32]. However, in our hands, there was a modest induction of T_H17 cells, accompanied by T_H1 cells as well, resulting in a mixed type-1/type-3 response (Supplementary Fig. 5a, b). In accordance, T_{REG} cell recruitment was similar among the major three subsets (Supplementary Fig. 5c, d). $Foxp3^{\Delta Roryt}$ mice mount a similar T_H1 and T_H17 cell response compared to $Foxp3^{Wt}$ controls (Supplementary Fig. 5e, f). SFB infection results in substantial $CD8^+$ T_{RM} cell establishment, but with reduced development in the absence of type-3 T_{REG} cells (Fig. 5a, b). However, the chronicity of SFB in the intestinal tract prohibits the further assessment of memory T-cell responses[32].

Influenza virus causes a strong type-1 response and establishment of $CD8^+$ T_{RM} cells in the lung, dependent on type-1 T_{REG} cells (Fig. 1). Upon infection, $Foxp3^{\Delta Roryt}$ and $Foxp3^{Wt}$ animals showed a similarly robust development of $CD8^+$ T_{RM} cells (Fig. 5c, d), in stark contrast to $Foxp3^{\Delta Tbx21}$ mice (Fig. 1i), indicating primarily a dependency on type-1 T_{REG} cells for $CD8^+$ T_{RM} cell development. This raised the question if *Aspergillus* infection, resulting in a strong type-3 response (Fig. 3), requires type-3 T_{REG} cells for optimal $CD8^+$ T_{RM} cell development. Upon *Aspergillus* infection the influx of $CD4^+$ T cells is similar between $Foxp3^{Wt}$ and $Foxp3^{\Delta Roryt}$ animals (Fig. 5e). However, the recruitment of T_{REG} cells is significantly lower (Fig. 5f), explained by the absence of type-3 T_{REG} cells (Fig. 5g). This is similar to our previous observations in type-1 infections in $Foxp3^{\Delta Tbx21}$ animals[14]. Genetic ablation of type-3 T_{REG} cells in $Foxp3^{\Delta Roryt}$ animals resulted in a marked reduction of $CD8^+$ T_{RM} development compared with $Foxp3^{Wt}$ animals (Fig. 5g, h). Importantly, and in line with previous results obtained with type-1 pathogens (Fig. 1)[14], co-transfer of control T_{REG} cells into type-3 T_{REG}–deficient hosts prior to a type-3 infection is able to restore $CD8^+$ T_{RM} cell development and numbers to the level seen in control mice, which also for type-3 responses relies on T_{REG} cell provision of TGFβ (Fig. 5i, Supplementary Fig. 5i).

Collectively, our data suggest that there appears to exist a matching of pathogen type and T_{REG} subset during type-1 and type-3 infections. Influenza, SFB and *Aspergillus*, show a dominant dependency of the equivalent T_{REG} subset for efficient $CD8^+$ T_{RM} cell development.

$CD8^+$ T_{RM} cell identity is maintained after infection

Eimeria vermiformis (Ev) is a small intestinal single-cell intracellular parasite that invades small intestine epithelial cells, it is mouse-specific and self-limiting, making it an ideal tool to study T_{RM} cell development[14]. It undergoes at least three rounds of asexual replication, each time bursting out of an infected epithelial cell to reach distal uninfected epithelial cells[33]. Its clearance depends on a type-1 inflammatory response, as we showed previously, and establishes type-1 T_{REG}-dependent $CD8^+$ T_{RM} cells[14]. We tested if the establishment of $CD8^+$ T_{RM} cells is inhibited by the absence of type-3 T_{REG} cells in $Foxp3^{\Delta Roryt}$ mice. $Foxp3^{\Delta Roryt}$ mice do show reduced $CD8^+$ T_{RM} cell development compared to $Foxp3^{Wt}$ controls, although the decrease is not as marked as in the absence of type-1 T_{REG}. (Fig. 6a, b)[14].

$CD8^+$ T cells are strongly associated with type-1 responses. We observed IFNγ-producing $CD8^+$ T cells also in type-2 and type-3 infections (Figs. 2c, d, 3c, d). Hence, we next questioned if, in a strong type-3 infection model such as *Aspergillus*, the subsequent $CD8^+$ T_{RM} cell establishment that is dependent on type-3 T_{REG} cells (Fig. 5e, f), shows any dependency on type-1 T_{REG} cells as is the case with Ev infection (Fig. 6a, b). In the case of *Aspergillus*, the absence of either type-3 or type-1 has marked effects on the generation of $CD8^+$ T_{RM} cells (Figs. 5e, f, 6c, d).

Since memory T cells are maintained to offer protection against future challenges, we wished to know if $CD8^+$ T_{RM} cells developed under polarising conditions of type-1 or type-3 infections reflected the original skewing. We assessed the endogenous $CD8^+$ T_{RM} cell population after the clearance of infection. Upon influenza infection, the established $CD8^+$ T_{RM} cells show a predominant skewing towards the original type-1 response, with the cells mainly able to produce IFNγ (Supplementary Fig. 6a–c). Upon an *Aspergillus* infection, the remaining $CD8^+$ T_{RM} cells are fewer and the skewing is less apparent. The recall response shows IL-17 production, in line with the initial type-3 immune response, but there is the presence of IFNγ-producing $CD8^+$ T_{RM} cells as well (Supplementary Fig. 6d–f). To analyse the polarisation of newly recruited $CD8^+$ T cells upon an *Aspergillus* challenge at the site of infection, we made use of our CD45.1 T-cell adoptive transfer model. The *Aspergillus* challenge shows a mixed type-1 and type-3 polarisation of established $CD8^+$ T_{RM} cells, indicating their polarisation is maintained after T_{RM} cell development (Fig. 6e–f). Furthermore, this model allows the assessment of the role of T_{REG} cell types on T_{RM} cell polarisation. Although type-1 and type-3 T_{REG} cells enhance the establishment of T_{RM} cells upon *Aspergillus* infection (Fig. 5), the absence of either type-1 or type-3 T_{REG} cells does not alter the polarisation toward the production of IFNγ or IL-17 (Fig. 6e, f).

Our data suggest that $CD8^+$ T_{RM} cell formation occurs predominantly during type-1 immune responses, largely depending on type-1 T_{REG} cell recruitment and action. Type-3 infections do give rise to $CD8^+$ T_{RM} cells as well, but these are more modest in numbers. Although there is preferential recruitment of infection-type-matching T_{REG} cells, there is redundancy between T_{REG} populations, especially when polarisation is less dominant. After establishment, $CD8^+$ T_{RM} cells maintain their original profile, determined by the infection type, after pathogen clearance.

https://doi.org/10.1038/s41467-023-41364-w

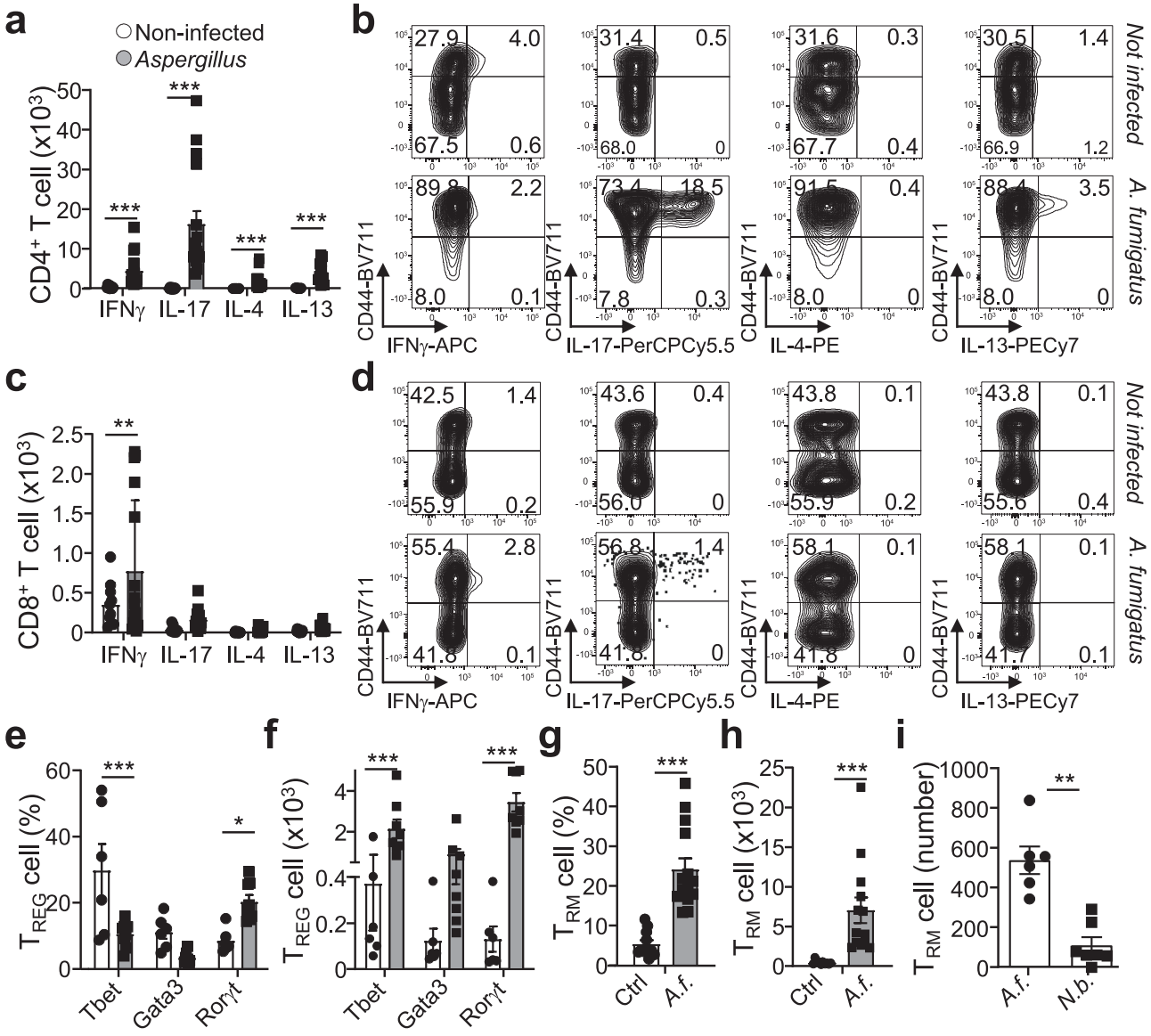

Fig. 3 | Type-3 Aspergillus fumigatus infection yields CD8 T-cell recruitment and TRM cell formation. Mice were intranasally challenged four times every 3 days with 10^6 spores of *Aspergillus fumigatus*. 10 days post-infection lungs were collected, and cells were isolated and analysed via flow cytometry for cytokine production, and T_{RM} cells. **a** Numbers of activated ($CD44^+$) $CD4^+$ T cells producing indicated cytokines, $p_{(\text{Non-infected vs } Aspergillus)}$: IFN-γ, $p = 0.005452$; IL-17, $p = 0.000733$; IL-4, $p = 0.007702$; IL-13, $p = 0.000005$, and **b** representative flow cytometry plots of cytokine production in $CD4^+$ T cells (non-infected $n = 10$, infected $n = 12$, $N = 4$). **c** Numbers of activated $CD8^+$ T cells producing indicated cytokines, $p_{(\text{Non-infected vs } Aspergillus)}$: IFN-γ, $p = 0.000951$, and **d** representative flow cytometry plots of cytokine production in $CD8^+$ T cells (non-infected $n = 10$, infected $n = 14$, $N = 4$). **e**, **f** T_{REG} cells from $Foxp3^{WT}$ mice were assessed for expression in **e** percentage, $p_{(\text{Non-infected vs } Aspergillus)}$: Tbet, $p = 0.018008$; RORγt, $p = 0.001023$, and **f** numbers, $p_{(\text{Non-infected vs } Aspergillus)}$: Tbet, $p = 0.022810$; RORγt, $p = 0.000093$, of the transcription factors Tbet, GATA-3 and RORγt in (non-infected $n = 6$, infected $n = 7$, $N = 3$). **g**, **h** Analysis of $CD69^+KLRG1^-$ $CD8^+$ T_{RM} cell (**g**) percentage, $p_{(\text{Non-infected vs } Aspergillus)} = 0.000017$, within the total $CD8^+$ T-cell population, and **h** number, $p_{(\text{Non-infected vs } Aspergillus)} = 0.002175$ in the lungs of non-infected (control) and infected mice ($n = 10$, non-infected, $n = 14$ infected, $N = 3$). **i** Comparison of transferred $CD8^{CD45.1}$ $CD69^+KLRG1^-$ $CD8^+$ T_{RM} cell numbers in the lungs upon *Nippostrongylus brasiliensis* (N.b.) or *Aspergillus fumigatus* (A.f.) infection, $p_{(\text{Aspergillus vs Nippostrongylus brasiliensis})} = 0.0012$, ($n = 7$, $N = 3$ for N.b.; $n = 6$ and $N = 3$ for A.f). Two-sided Mann-Whitney analysis was applied to compare the differences between groups. Data is presented as bars of mean ± SEM with single data points.

Discussion

Non-lymphoid tissue immunity is important to guard against reinfection, local containment of invaders and to reduce the chance of systemic dissemination[34]. This is established after primary infection and is of great interest for vaccine strategies. T_{REG} cells are a critical component in the management of immune responses, maintaining self-tolerance and homoeostasis. Different populations of T_{REG} cells exist and co-localise with the corresponding $CD4^+$ Th cell subsets, with similar transcriptional programmes and associated expression of chemokine receptors[27,35,36]. Our previous data showed the requirement of type-1 T_{REG} cell recruitment to the site of inflammation to release and make available TGFβ, thereby facilitating $CD8^+$ T_{RM} cell development. The work focussed on an intestinal intracellular parasite infection, *Eimeria vermiformis*, invoking a type-1 dominated response with $CD8^+$ T_{RM} cell development dependent on type-1, Tbet- and CXCR3-expressing, T_{REG} cells[14]. Mirroring of transcription programmes and chemokine receptor expression raised the question that particular T_{REG} subsets may control immune responses within the context of the pathogen encountered. This suggests that the development of $CD8^+$ T_{RM} cells may require a match between type of infection and T_{REG} subset to be recruited[22].

Localised infections result in strong $CD8^+$ T_{RM} cell development, require inflammation-mediated lymphocyte trafficking and the

https://doi.org/10.1038/s41467-023-41364-w

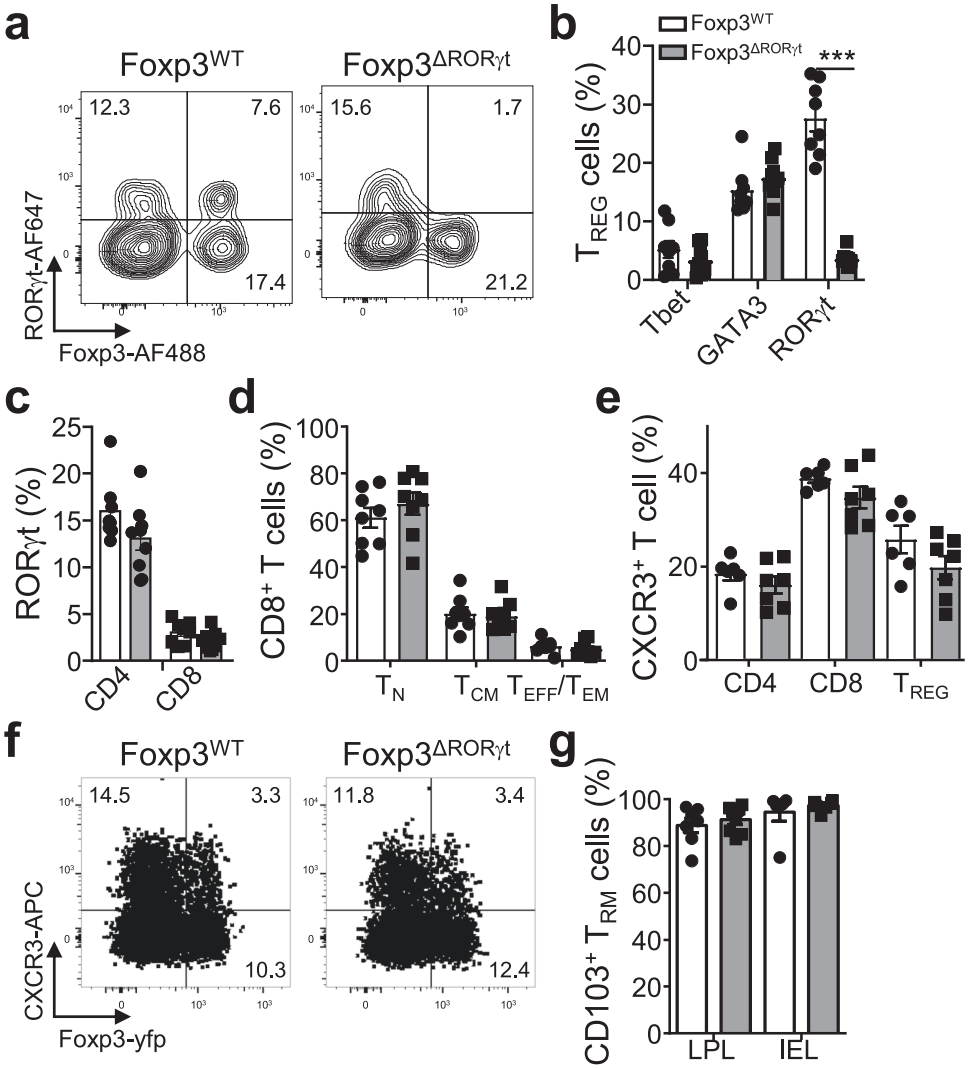

Fig. 4 | Type-3 TREG cells are ablated in Foxp3-CreeYFP RORγtfl/fl mice. Foxp3^{WT} and Foxp3$^{\Delta RORγt}$ mice were analysed at steady-state for T_{REG}, CD4$^+$, and CD8$^+$ T cells in lung, spleen, small intestine lamina propria lymphocytes (LPL), and small intestine intraepithelial lymphocytes (IEL). **a** Representative flow plot of RORγt expression in LPL T_{REG} cells in both mouse lines. **b** Percentage of LPL T_{REG} cells expressing Tbet, GATA-3 or RORγt, $p_{(Foxp3WT\ vs\ Foxp3\Delta RORγt)} < 0.000001$, (Foxp3^{WT} $n = 8$, Foxp3$^{\Delta RORγt}$ $n = 9$, $N = 3$). **c** Percentage of RORγt expression in CD4$^+$ and CD8$^+$ LPL (Foxp3^{WT} $n = 8$, Foxp3$^{\Delta RORγt}$ $n = 9$, $N = 3$). **d**–**f** CD8$^+$ T-cell proportions in the spleen were assessed for **d** naive (T_N CD44$^-$CD62L$^+$), central memory (T_{CM}, CD44$^+$CD62L$^+$) and effector memory/effector (T_{EM}/T_{EFF}, CD44$^+$CD62L$^-$) and **e** for CXCR3 expression on CD4$^+$, CD8 and T_{REG} cells, with **f** representative flow plot ($n = 8$, $N = 3$). **g** Percentage of CD69$^+$KLRG1$^-$CD103$^+$ CD8$^+$ T_{RM} cell in small intestine LPL and IEL in both mouse lines (LPL Foxp3^{WT} $n = 7$, Foxp3$^{\Delta RORγt}$ $n = 8$, $N = 3$; IELs $n = 6$, $N = 2$). Two-sided Mann–Whitney analysis was applied to compare the differences between groups. Data is presented as bars of mean ± SEM with single data points.

cognate antigen to be present in the local microenvironment[14,34,37,38]. Our results are obtained using three distinct infection models in the lungs. In each of the models, CD4$^+$ T cells are recruited to the site of inflammation, and each type of infection is dominated by the corresponding T_H cell subset, in numbers and proportions; Influenza by T_H1 cells (IFNγ), *N. brasiliensis* by T_H2 cells (IL-4, IL-13), and *A. fumigatus* by T_H17 cells (IL-17). A potential limitation of our analysis is that we did not in vivo label the studied cells, a method used to identify circulating cells. However, this method has some disadvantages as it does not address migration properties and, in a highly vascular organ such as the lungs, the inflammatory context might result in tissue permeability and affect the results[39].

We tested the role of type-3 T_{REG} cells in the establishment of CD8$^+$ T_{RM} cells after a type-3 infection by genetically removing them using Foxp3$^{\Delta Rorγt}$ animals. We successfully used this approach with Foxp3$^{\Delta Tbx21}$ animals[14]. In Foxp3$^{\Delta Rorγt}$ animals, the total number of T_{REG} cells, including type-1 T_{REG} cells that contribute to CD8$^+$ T_{RM} cell development, T_H17 cells, and CD8$^+$ T cells expressing Rorγt were not altered. This confirms that the Foxp3-Cre-driven deletion is T_{REG}-specific and attests to the careful genotyping of mice used. Conform our previous results in the small intestine[14], predominantly type-1 T_{REG} cells are recruited upon a viral infection in the lung, which are required to enhance the establishment of CD8$^+$ T_{RM} cells. CD8 T cells are also recruited to the site of the influenza infection and are nearly exclusively IFNγ-producers. Although we observe a robust T_H2 cell response upon *N. brasiliensis* infection, and although more T_{REG} cells are recruited, we did not see a predominance of type-2 T_{REG} cells at the site of infection. In addition, CD8$^+$ T cells are marginally recruited to, and activated at, the site of infection, although the presence of more endogenous CD8$^+$ T_{RM} cells was observed. It is not clear if these cells are an expansion of the local CD8$^+$ T_{RM} cell population responding to a local inflammation or if these are pathogen-specific. However, using CD45.1 adoptive transfers, it is clear that few naïve CD8$^+$ T cells are recruited to the site of infection, while CD4$^+$ T cells are. The cytokine expression profile of CD8$^+$ T cells did not differ from non-infected controls, and the characteristic type-2 cytokines IL-4 and IL-13 were not detected. CD8$^+$ T cells are not

https://doi.org/10.1038/s41467-023-41364-w

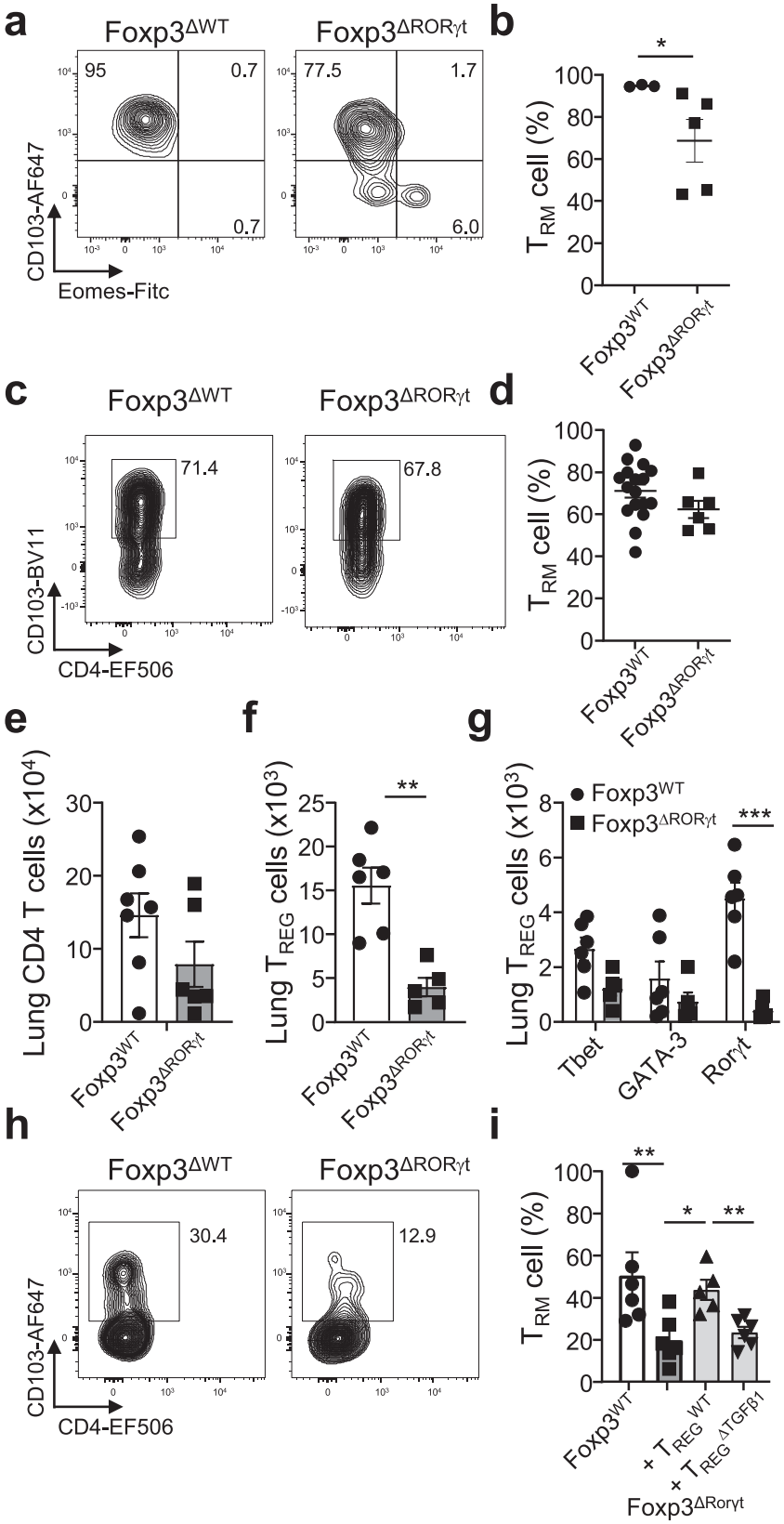

associated with type-2 or anti-helminth responses[40]. There are suggestions that helminths may themselves reduce the $CD8^+$ T-cell response[41]. Therefore, our results may be applicable to helminth-induced type-2 responses but not represent allergic responses.

Type-3-dominated infections, represented by *A. fumigatus* and SFB, do result in preferential recruitment of type-3 T_{REG} cells as well as the recruitment of $CD8^+$ T cells. However, and in contrast to $CD4^+$ T cells, the $CD8^+$ T cells recruited are less numerous compared to influenza. IL-17-producing $CD8^+$ T cells are present after type-3 infection, but constitute a small population. $CD8^+$ T_{RM} cell development does take place, but is not as efficient as observed during a type-1 response. In contrast to $Foxp3^{\Delta Tbx21}$ animals in which we observe a

https://doi.org/10.1038/s41467-023-41364-w

Fig. 5 | Depletion of Type-3 TREG cells reduces TRM cell development in type-3 infections. a, **b** In Foxp3^{WT} and Foxp3$^{\Delta ROR\gamma t}$ mice, CD45.1$^+$ CD8$^+$ T cells were transferred one day prior to infection with 100 mg of segmented filamentous bacteria (SFB)-containing feces, organs were assessed for their T_{RM} cell phenotype (CD69$^+$Eomes$^-$CD103$^+$) 14 days later. Small intestine LPL were collected and assessed for the T-cell phenotype of CD45.1$^+$ CD8$^+$ T_{RM} cells. **a** Representative flow cytometry plots and **b** percentages of T_{RM} cells, $p_{(Foxp3WT\ vs\ Foxp3\Delta RORγt)} = 0.0357$, (Foxp3^{WT} $n = 3$, Foxp3$^{\Delta ROR\gamma t}$ $n = 5$, $N = 3$). **c**, **d** Intranasal challenge with 1000 PFU of Influenza X-31 strain (H3N2). Lungs were collected and transferred T cells were analysed. **c** Representative flow cytometry plots of T_{RM} cells within transferred T cells and **d** percentages of T_{RM} cells in indicated mouse lines (Foxp3^{WT} $n = 17$, Foxp3$^{\Delta ROR\gamma t}$ $n = 6$, $N = 4$). **e**–**g** Mice were infected by four intranasal challenges with 10^6 spores of *Aspergillus fumigatus*. Lungs were collected and **e** total CD4$^+$ T cells (Foxp3^{WT} $n = 7$, Foxp3$^{\Delta ROR\gamma t}$ $n = 6$, $N = 3$), **f** total T_{REG} cells, $p_{(Foxp3WT\ vs\ Foxp3\Delta RORγt)}$=0.0043, and **g** subsets of T_{REG} cells based on their transcription factor expression, $p_{(Foxp3WT\ vs\ Foxp3\Delta RORγt)} = 0.000001$, were analysed (Foxp3^{WT} $n = 6$ Foxp3$^{\Delta ROR\gamma t}$ $n = 5$, $N = 3$). **h**, **i** Mice were transferred with indicated condition receiving control or TGFβ1–deficient T_{REG} cells prior to the first of four intranasal challenges with 10^6 spores of *Aspergillus fumigatus*. Lungs were collected and transferred CD45.1 CD8 T cells were analysed. **h** Representative flow cytometry plots of T_{RM} cells within transferred CD45.1 CD8 T cells and **i** percentages of T_{RM} cells in all conditions, $p_{(Foxp3WT\ vs\ Foxp3\Delta RORγt)} = 0.0087$, $p_{(Foxp3\Delta RORγt\ vs\ Foxp3\Delta RORγt+WT\ Tregs)} = 0.0173$, $p_{(Foxp3\Delta RORγt\ vs\ Foxp3\Delta RORγt+Treg\Delta TGFβ1)} = 0.0043$ (Foxp3^{WT}; Foxp3$^{\Delta ROR\gamma t}$ $n = 6$, $N = 4$; Foxp3$^{\Delta ROR\gamma t}$ + $T_{REG}{}^{WT}$ $n = 5$, $N = 2$; Foxp3$^{\Delta ROR\gamma t}$ + $T_{REG}{}^{\Delta TGFβ1}$ $n = 5$, $N = 2$). Multiple unpaired *t* test was used for **g**, other panels two-sided Mann-Whitney analysis was applied to compare groups. Data is presented as bars of mean ± SEM with single data points.

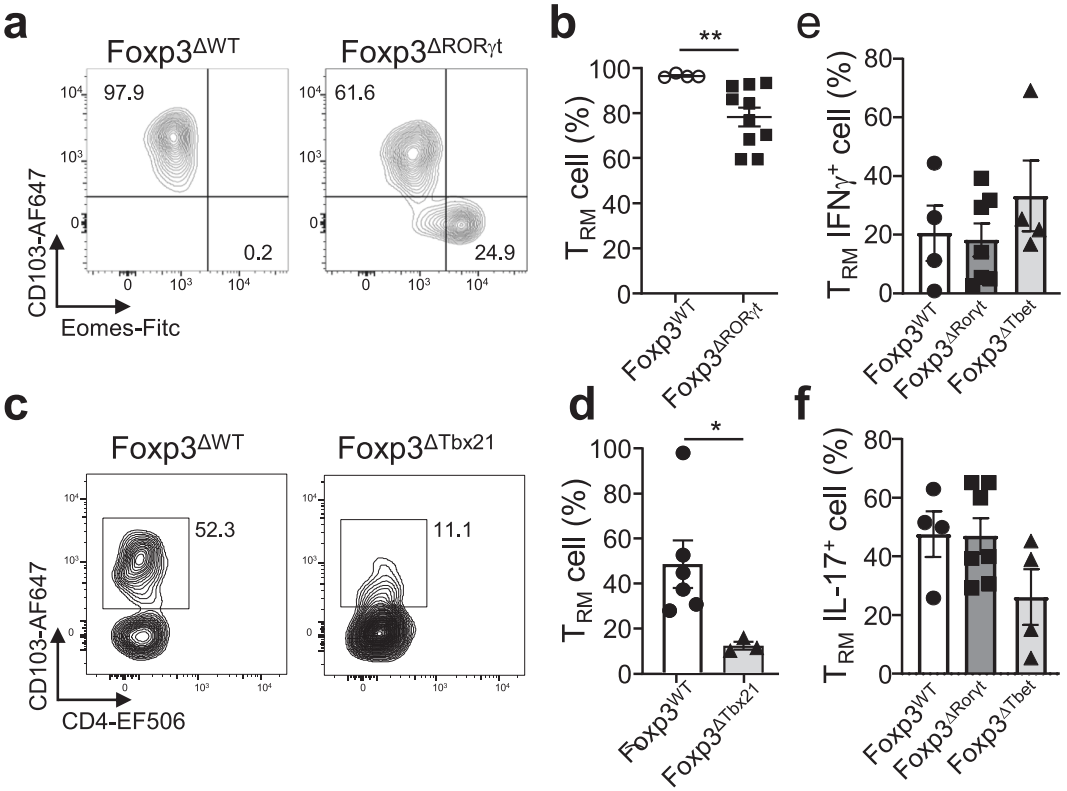

Fig. 6 | Type-1 and type-3 TREG cells enhance TRM cell development, the identity of which are maintained. Mice were transferred with CD45.1$^+$ CD8$^+$ T cells one day prior to oral gavage infection. 14 days after transplant, tissues were collected and assessed for their T_{RM} phenotype. **a**, **b** Infection with 5000 oocysts of *Eimeria vermiformis*, **a** representative flow cytometry plots T_{RM} cells (CD69$^+$Eomes$^-$CD103$^+$) and **b** percentages of T_{RM} cells in both mouse lines, $p_{(Foxp3WT\ vs\ Foxp3\Delta RORγt)} = 0.0020$, (Foxp3^{WT} $n = 4$, Foxp3$^{\Delta ROR\gamma t}$ $n = 10$, $N = 3$). **c**, **d** Mice were challenged four times intranasally with 10^6 spores of *Aspergillus fumigatus*. Lungs were collected and transferred T cells were analysed, **c** representative flow cytometry plots of T_{RM} cells and **d** percentages of T_{RM} cells in both mouse lines, $p_{(Foxp3WT\ vs\ Foxp3\Delta Tbet)} = 0.0238$ (Foxp3^{WT} $n = 6$, $N = 4$, Foxp3$^{\Delta Tbx21}$ $n = 3$, $N = 3$). **e**, **f** Mice were transferred with CD45.1 CD8 T cells prior to the first of four intranasal challenges with 10^6 spores of *Aspergillus fumigatus*. Lungs were collected and transferred CD45.1 CD8$^+$ T_{RM} cells were analysed for **e** IFNγ or **f** IL-17 production (Foxp3^{WT} $n = 4$, Foxp3$^{\Delta ROR\gamma t}$ $n = 7$, Foxp3$^{\Delta Tbx21}$ $n = 4$, $N = 3$). Two-sided Mann–Whitney analysis was applied to compare groups. Data is presented as bars of mean ± SEM with single data points.

marked decrease in CD8$^+$ T_{RM} cells under steady-state conditions without known infection, Foxp3$^{\Delta Rorγt}$ animals have numbers of CD8$^+$ T_{RM} cells comparable to controls. This indicates that type-3 T_{REG} cell recruitment does not make a critical contribution to the overall development of CD8$^+$ T_{RM} cells. Upon infection with *A. fumigatus* or SFBs, however, the absence of type-3 T_{REG} cells makes CD8$^+$ T_{RM} cell development less efficient.

We confirm that the development of CD8$^+$ T_{RM} cells during a type-1 infection, such as influenza, does not depend on type-3 T_{REG} cells but on type-1 T_{REG} cell recruitment exclusively. Less polarised responses or non-type-1 dominated infections are less dependent on specific T_{REG} subset recruitment to facilitate CD8$^+$ T_{RM} cell development. This is in agreement with the T cells detected during the *A. fumigatus* or SFB infection showing a type-1 and type-3 identity, hence relying on type-1 and type-3 T_{REG} cell recruitment for CD8$^+$ T_{RM} cell establishment. Infections are often a mixed response with type-1 responses playing an important role in most[42]. This may reflect the involvement of CD8$^+$ T cells, which show an overwhelming type-1 dominated response. In accordance, the development of CD8$^+$ T_{RM} cells during type-3 responses is not exclusively dependent on type-3 T_{REG} cell recruitment, but also on type-1 T_{REG} cells. However, the polarisation of CD8$^+$ T_{RM} cells is determined by the infection and not by the recruitment of type-1 or type-3 T_{REG} cells. In the context of any invader, the establishment of a tissue-resident T-cell memory pool

will be an advantage to locally contain the infection, independent of antigen specificity[43].

The functional relevance of mismatched CD8$^+$ T_{RM} cells during a reinfection is speculative but type-3 responses are flexible and can be converted to give rise to type-1 cells[44]. Although largely observed on CD4$^+$ T cells, a mixed type-1/-3 response can be beneficial to reduce pathogen load and pathology in subsequent infections[45–49]. In addition, tissue repair can be enhanced by type-2 responses and type-3 CD8$^+$ T_{RM} cells have been reported in the context of signals from injury and exposure to inflammatory mediators to release type-2 cytokines[50]. The physiological and clinical relevance of this mixed response, especially for CD8$^+$ T_{RM} cells, is currently not clear but a subject for future investigation.

In summary, we extend previous work that T_{REG} cells, critical in preventing autoimmunity and immunopathology, have an important role in efficiently generating tissue-resident memory T cells from effector or memory precursors. We show that type-2 helminth infections are unlikely to result in robust de novo CD8$^+$ T_{RM} cell formation. Type-3 infections result in CD8$^+$ T_{RM} cell development, but less robust than type-1 infections. Type-1 T_{REG} cell recruitment is required for CD8$^+$ T_{RM} cell development during type-1 infections, although type-3 T_{REG} cells may assist in less type-1 dominated responses, resulting in a predominantly IFNγ–producing CD8$^+$ T_{RM} cell population. During type-3 infection, both type-1 and -3 T_{REG} cells play an important role, resulting in the establishment of a CD8$^+$ T_{RM} cell population containing a mix of IFNγ- and IL-17-producing cells. Excluding helminths, independently of the type of pathogen encountered, CD8$^+$ T_{RM} cells are generated, offering enhanced protection against future challenges.

Methods

Mice

C57BL/6 J CD45.1 mice were purchased from Charles River, France. Tbx21$^{fl/fl}$ (Tbx21^{tm2Srnr}) were kindly provided by Dr. Steven Reiner[51], Foxp3eYFP-Cre (Foxp3$^{tm4(YFP/icre)Ayr}$) was kindly provided by Dr. Alexander Rudensky[52], Rosa26-tdRFP was kindly provided by Dr. Hans Jörg Fehling[53]. RORγt$^{fl/fl}$ mice were obtained on Jackson Laboratories, Foxp3eYFP-Cre TGFβ1$^{-/-}$ mice were kindly provided by Dr. Julien Marie[14]. Mice were bred at the Instituto de Medicina Molecular, Lisbon, Portugal. Male and female mice, aged and sex-matched, at 12–25 weeks of age were used. Animals were housed in IVC cages with temperature-controlled conditions under a 12-h light/dark cycle with free access to drinking water and food. All mice were kept in specific pathogen-free conditions. All mice in the Foxp3eYFP-Cre Rosa26-tdRFP lines were stringently genotyped by PCR and those in which a knockout allele was detected were discarded (~20%). In addition, mice were counter-screened for inappropriate expression of RFP in relation to eYFP (~10% discarded). All animal experimentation complied with regulations and guidelines of, and was approved by, the Direção-Geral de Alimentação e Veterinária Portugal and the local ethical review committee (Orbea).

Cell isolation

ntestine was flushed with PBS to remove contents and opened longitudinally. After cutting into 1 cm pieces, it was incubated in PBS containing 20 mM Hepes, 100 U/ml penicillin, 100 μg/ml streptomycin, 1 mM Pyruvate, 10% FCS, 100 μg/ml polymyxin B and 10 mM EDTA for 30 min at 37 °C while shaking to release IELs. IEL single-cell suspensions were further purified using 37.5% isotonic Percoll. To isolate LPLs, intestinal tissue was then digested in IMDM medium containing 0.5 mg/ml of Collagenase D (Roche) and 0.2 mg/ml of DNaseI (Roche) for 25 min at 37 °C while shaking.

Lungs were perfused with 20 mL of PBS before being shredded in small pieces with scissors and digested in IMDM medium containing 5% FBS and 0.5 mg/ml Collagenase D, 37 °C during 30 min while shaking. The cell suspension containing the lymphocytes was passed through a 50 μm cell strainer, incubated for 2 min in ACK solution, and lymphocytes were obtained after a 6-min wash with PBS at 500 g centrifugation.

Adoptive cell transfers

CD8α$^+$ T cells and/or CD25$^+$ cells (T_{REG} cells) were purified from a single-cell suspension of spleen and lymph nodes. Briefly, cells were labelled with anti-CD8a-APC or anti-CD25-APC antibodies and selected with anti-APC MACS microbeads, according to the manufacturer's instructions. After counting, purity was determined by flow cytometry, and cell numbers were adjusted. To ensure a wide TCR diversity in the population transferred a minimum of 2×10^6 CD8$^+$ T cells were used. Some of the recipient mice received in addition $0.6–1 \times 10^6$ T_{REG} cells. Infection was performed one day after cell transfer (day 0).

Influenza X-31 preparation and infection

Reverse genetics A/X-31 (PR8-HK4 and 6) were used as model viruses. Reverse genetics derived chimeric PR8 containing the segment 4 from A/Hong Kong/1/1968, seg4-HK68 (PR8-HK4), or the segment 6 (PR8-HK6) were produced as previously described[54–56]. pDual plasmids were a kind gift from Dr. Ron Fouchier (Erasmus MC, Netherlands). PR8 NA-E229A[57] was generated by reverse genetics after site-directed mutagenesis of pDual::segment 6. All viruses were amplified in embryonated chicken eggs and titrated using plaque assay as previously described[58,59]. A viral load of 1000 PFU was administered in 30 μL PBS intranasally to mice. Mouse weight was monitored daily during the experiment to certify welfare, with mice going lower than 25% initial weight being sacrificed.

Eimeria vermiformis infection

Animals were infected with *Eimeria vermiformis* (Ev) as previously described in detail[33]. Briefly, oocysts were washed three times with deionized water, floated in sodium hypochloride and counted using a Fuchs-Rosenthal chamber. Mice received 5000 oocysts of *E. vermiformis* by oral gavage in 100 μl of water.

N. brasiliensis infection

N. brasiliensis worms were propagated as previously described[30]. Infective L3 larvae were kindly provided by Brian Chan at Dr Judith E Allen's laboratory. Briefly, the larvae were obtained by cutting the filter paper in which they were provided around the borders (~0.5 cm), emerging it around gauze in a Falcon tube with 40 mL of PBS at 37 °C for 10 min (Baermann's method). After this, larvae were allowed to pool down by gravity for 10 min, with the bottom 10–15 mL containing them being transferred to a 15 mL tube. The larvae were then purified by performing three washes at 168 g with minimum break. Mice were then injected with 300 L3s subcutaneously.

A. fumigatus preparation and infection

Fungal isolate *A. fumigatus* strain Af293 was purchased from the Fungal Genetics Stock Center (Kansas City, MO, United States). The fungal strain was cultivated on T-flasks containing sabouraud dextrose agar (SDA). Cultures were incubated in the dark, for 3–4 days, at 37 °C. Asexual spores (conidia) were harvested using glass beads and a saline solution B (0.85% NaCl, 0.1% Tween-20), washed twice with a saline solution A (0.85% NaCl), and collected after passing through three layers of miracloth filter. The harvested conidia were resuspended in a phosphate-buffered saline solution (0.01 M phosphate buffer, 0.0027 M potassium chloride, 0.137 M sodium chloride, pH 7.4), and kept at 4 °C until mice infection (same day). Prior to infection, conidia were counted with a hemacytometer and subsequently resuspended to a concentration of 3.3×10^7 conidia/mL^{-1},

30 µL were used for mice infection (106 conidia). Mice were submitted to 4 intranasal challenges with 10^6 conidia every 3 days over 2 weeks.

SFB fecal transplant

SFB-containing feces were kindly provided by Dr. Gérard Eberl at Pasteur Institute, Paris. Fecal pellets were collected and kept at −20 °C to maintain integral microbiota. On the day of the fecal transplant, feces were defrosted, mashed, and suspended in filtered tap water at a concentration of 100 mg/mL. Mice then received a fecal transplant of 200 µL of this suspension by oral gavage.

Flow cytometry

Single-cell suspensions from spleen, intestine, and lung were prepared and stained with antibodies (Supplementary Table 1), according to the agreed standards[60]. For intracellular cytokine staining, cells were pre-stimulated with PDBU (Phorbol 12,13-dibutyrate) (0.5 µg/mL) and ionomycin (0.5 µg/mL), in the presence of Brefeldin A (2 µg/mL) (all from Sigma) for 2 h at 37 °C. Samples were run on a Fortessa X20 cytometer (BD Biosciences) and analysed with FlowJo X software (TreeStar) (Supplementary Fig. 7).

Statistical analysis

In the present work, statistical analyses were performed using GraphPad Prism Software (GraphPad Prism version 9 for Windows, GraphPad Software, San Diego, California USA), details described in each figure legend where applicable. *N* denotes the number of independent biological repeats and *n* the total number of samples (mice). Error bars represent S.E.M. Mann–Whitney analysis was applied to compare ranks between two groups with a *p* value of 0.05. $^*P < 0.05$, $^{**}P < 0.01$, $^{***}P < 0.001$.

Reporting summary

Further information on research design is available in the Nature Portfolio Reporting Summary linked to this article.

Data availability

The authors declare that data supporting the findings of this study are available within the paper and its supplementary information files. Source data are provided with this paper. Additional materials or data that support the findings of this study are available from the corresponding authors. Source data are provided with this paper.

References

1. Konjar, S., Ferreira, C., Blankenhaus, B. & Veldhoen, M. Intestinal barrier interactions with specialized CD8 T cells. *Front. Immunol.* **8**, 1281 (2017).
2. Masopust, D., Vezys, V., Marzo, A. L. & Lefrancois, L. Preferential localization of effector memory cells in nonlymphoid tissue. *Science* **291**, 2413–2417 (2001).
3. Reinhardt, R. L., Khoruts, A., Merica, R., Zell, T. & Jenkins, M. K. Visualizing the generation of memory CD4 T cells in the whole body. *Nature* **410**, 101–105 (2001).
4. Konjar, S., Ficht, X., Iannacone, M. & Veldhoen, M. Heterogeneity of tissue resident memory T cells. *Immunol. Lett.* **245**, 1–7 (2022).
5. Shiow, L. R. et al. CD69 acts downstream of interferon-alpha/beta to inhibit S1P1 and lymphocyte egress from lymphoid organs. *Nature* **440**, 540–544 (2006).
6. Skon, C. N. et al. Transcriptional downregulation of S1pr1 is required for the establishment of resident memory CD8+ T cells. *Nat. Immunol.* **14**, 1285–1293 (2013).
7. Mackay, L. K. et al. Cutting edge: CD69 interference with sphingosine-1-phosphate receptor function regulates peripheral T-cell retention. *J. Immunol.* **194**, 2059–2063 (2015).
8. Walsh, D. A. et al. The functional requirement for CD69 in establishment of resident memory CD8(+) T cells varies with tissue location. *J. Immunol.* **203**, 946–955 (2019).
9. Ray, S. J. et al. The collagen binding alpha1beta1 integrin VLA-1 regulates CD8 T cell-mediated immune protection against heterologous influenza infection. *Immunity* **20**, 167–179 (2004).
10. Mackay, L. K. et al. The developmental pathway for CD103(+)CD8+ tissue-resident memory T cells of skin. *Nat. Immunol.* **14**, 1294–1301 (2013).
11. Cheuk, S. et al. CD49a expression defines tissue-resident CD8(+) T cells poised for cytotoxic function in human skin. *Immunity* **46**, 287–300 (2017).
12. Reilly, E. C. et al. TRM integrins CD103 and CD49a differentially support adherence and motility after resolution of influenza virus infection. *Proc. Natl. Acad. Sci. USA* **117**, 12306–12314 (2020).
13. Herndler-Brandstetter, D. et al. KLRG1(+) effector CD8(+) T cells lose KLRG1, differentiate into all memory T-cell lineages, and convey enhanced protective. *Immunity* **48**, 716–729.e718 (2018).
14. Ferreira, C. et al. Type 1 Treg cells promote the generation of CD8(+) tissue-resident memory T cells. *Nat. Immunol.* **21**, 766–776 (2020).
15. Bottois, H. et al. KLRG1 and CD103 expressions define distinct intestinal tissue-resident memory CD8 T-cell subsets modulated in Crohn's disease. *Front. Immunol.* **11**, 896 (2020).
16. Mackay, L. K. et al. T-box transcription factors combine with the cytokines TGF-beta and IL-15 to control tissue-resident memory T-cell fate. *Immunity* **43**, 1101–1111 (2015).
17. Zaid, A. et al. Persistence of skin-resident memory T cells within an epidermal niche. *Proc. Natl. Acad. Sci. USA* **111**, 5307–5312 (2014).
18. Mackay, L. K. et al. Hobit and Blimp1 instruct a universal transcriptional program of tissue residency in lymphocytes. *Science* **352**, 459–463 (2016).
19. Konjar, S. et al. Mitochondria maintain controlled activation state of epithelial-resident T lymphocytes. *Sci. Immunol.* **3**, eaan2543 (2018).
20. Konjar, S. & Veldhoen, M. Dynamic metabolic state of tissue resident CD8 T cells. *Front. Immunol.* **10**, 1683 (2019).
21. Ariotti, S. et al. Tissue-resident memory CD8+ T cells continuously patrol skin epithelia to quickly recognize local antigen. *Proc. Natl. Acad. Sci. USA* **109**, 19739–19744 (2012).
22. Barros, L., Ferreira, C. & Veldhoen, M. The fellowship of regulatory and tissue-resident memory cells. *Mucosal Immunol.* **15**, 64–73 (2022).
23. de Goer de Herve, M. G., Jaafoura, S., Vallee, M. & Taoufik, Y. FoxP3(+) regulatory CD4 T cells control the generation of functional CD8 memory. *Nat. Commun.* **3**, 986 (2012).
24. Pace, L. et al. Regulatory T cells increase the avidity of primary CD8+ T-cell responses and promote memory. *Science* **338**, 532–536 (2012).
25. Laidlaw, B. J. et al. Production of IL-10 by CD4(+) regulatory T cells during the resolution of infection promotes the maturation of memory CD8(+) T cells. *Nat. Immunol.* **16**, 871–879 (2015).
26. Miyao, T. et al. Plasticity of Foxp3(+) T cells reflects promiscuous Foxp3 expression in conventional T cells but not reprogramming of regulatory T cells. *Immunity* **36**, 262–275 (2012).
27. Duhen, T., Duhen, R., Lanzavecchia, A., Sallusto, F. & Campbell, D. J. Functionally distinct subsets of human FOXP3+ Treg cells that phenotypically mirror effector Th cells. *Blood* **119**, 4430–4440 (2012).
28. Levine, A. G. et al. Stability and function of regulatory T cells expressing the transcription factor T-bet. *Nature* **546**, 421–425 (2017).
29. Harvie, M. et al. The lung is an important site for priming CD4 T-cell-mediated protective immunity against gastrointestinal helminth parasites. *Infect. Immun.* **78**, 3753–3762 (2010).

30. Lawrence, R. A., Gray, C. A., Osborne, J. & Maizels, R. M. Nippostrongylus brasiliensis: cytokine responses and nematode expulsion in normal and IL-4-deficient mice. *Exp. Parasitol.* **84**, 65–73 (1996).
31. Zelante, T. et al. IL-23 and the Th17 pathway promote inflammation and impair antifungal immune resistance. *Eur. J. Immunol.* **37**, 2695–2706 (2007).
32. Ivanov, I. I. et al. Induction of intestinal Th17 cells by segmented filamentous bacteria. *Cell* **139**, 485–498 (2009).
33. Figueiredo-Campos P, Ferreira C, Blankenhaus B, Veldhoen M. Eimeria vermiformis infection model of murine small intestine. *Bio. Protoc.* **8**, e3122 (2018).
34. Gebhardt, T. et al. Memory T cells in nonlymphoid tissue that provide enhanced local immunity during infection with herpes simplex virus. *Nat. Immunol.* **10**, 524–530 (2009).
35. Chaudhry, A. et al. CD4+ regulatory T cells control TH17 responses in a Stat3-dependent manner. *Science* **326**, 986–991 (2009).
36. Koch, M. A. et al. T-bet(+) Treg cells undergo abortive Th1 cell differentiation due to impaired expression of IL-12 receptor beta2. *Immunity* **37**, 501–510 (2012).
37. Mackay, L. K. et al. Long-lived epithelial immunity by tissue-resident memory T (TRM) cells in the absence of persisting local antigen presentation. *Proc. Natl. Acad. Sci. USA* **109**, 7037–7042 (2012).
38. Khan, T. N., Mooster, J. L., Kilgore, A. M., Osborn, J. F. & Nolz, J. C. Local antigen in nonlymphoid tissue promotes resident memory CD8+ T-cell formation during viral infection. *J. Exp. Med.* **213**, 951–966 (2016).
39. Anderson, K. G. et al. Intravascular staining for discrimination of vascular and tissue leukocytes. *Nat. Protoc.* **9**, 209–222 (2014).
40. Wong, P. & Pamer, E. G. CD8 T-cell responses to infectious pathogens. *Annu. Rev. Immunol.* **21**, 29–70 (2003).
41. Actor, J. K. et al. Helminth infection results in decreased virus-specific CD8+ cytotoxic T-cell and Th1 cytokine responses as well as delayed virus clearance. *Proc. Natl. Acad. Sci. USA* **90**, 948–952 (1993).
42. Kiner, E. et al. Gut CD4(+) T-cell phenotypes are a continuum molded by microbes, not by TH archetypes. *Nat. Immunol.* **22**, 216–228 (2021).
43. Ariotti, S. et al. T-cell memory. Skin-resident memory CD8(+) T cells trigger a state of tissue-wide pathogen alert. *Science* **346**, 101–105 (2014).
44. Hirota, K. et al. Fate mapping of IL-17-producing T cells in inflammatory responses. *Nat. Immunol.* **12**, 255–263 (2011).
45. Bai, H. et al. IL-17/Th17 promotes type 1 T-cell immunity against pulmonary intracellular bacterial infection through modulating dendritic cell function. *J. Immunol.* **183**, 5886–5895 (2009).
46. Borkner, L., Curham, L. M., Wilk, M. M., Moran, B. & Mills, K. H. G. IL-17 mediates protective immunity against nasal infection with Bordetella pertussis by mobilizing neutrophils, especially Siglec-F(+) neutrophils. *Mucosal Immunol.* **14**, 1183–1202 (2021).
47. Nguyen, N. et al. Th1/Th17 T-cell tissue-resident immunity increases protection, but is not required in a vaccine strategy against genital infection with chlamydia trachomatis. *Front. Immunol.* **12**, 790463 (2021).
48. Dhume, K. et al. Bona fide Th17 cells without Th1 functional plasticity protect against influenza. *J. Immunol.* **208**, 1998–2007 (2022).
49. Omokanye, A. et al. Clonotypic analysis of protective influenza M2e-specific lung resident Th17 memory cells reveals extensive functional diversity. *Mucosal Immunol.* **15**, 717–729 (2022).
50. Harrison O.J. et al. Commensal-specific T-cell plasticity promotes rapid tissue adaptation to injury. *Science* **363**, eaat6280 (2019).
51. Intlekofer, A. M. et al. Requirement for T-bet in the aberrant differentiation of unhelped memory CD8+ T cells. *J. Exp. Med.* **204**, 2015–2021 (2007).
52. Rubtsov, Y. P. et al. Regulatory T cell-derived interleukin-10 limits inflammation at environmental interfaces. *Immunity* **28**, 546–558 (2008).
53. Luche, H., Weber, O., Nageswara Rao, T., Blum, C. & Fehling, H. J. Faithful activation of an extra-bright red fluorescent protein in "knock-in" Cre-reporter mice ideally suited for lineage tracing studies. *Eur. J. Immunol.* **37**, 43–53 (2007).
54. Marjuki, H. et al. An investigational antiviral drug, DAS181, effectively inhibits replication of zoonotic influenza A virus subtype H7N9 and protects mice from lethality. *J. Infect. Dis.* **210**, 435–440 (2014).
55. Matrosovich, M., Matrosovich, T., Garten, W. & Klenk, H. D. New low-viscosity overlay medium for viral plaque assays. *Virol. J.* **3**, 63 (2006).
56. Moskovich, O. & Fishelson, Z. Quantification of complement C5b-9 binding to cells by flow cytometry. *Methods Mol. Biol.* **1100**, 103–108 (2014).
57. Luster, A. D. & Leder, P. IP-10, a -C-X-C- chemokine, elicits a potent thymus-dependent antitumor response in vivo. *J. Exp. Med.* **178**, 1057–1065 (1993).
58. Miwa, T. et al. Deletion of decay-accelerating factor (CD55) exacerbates autoimmune disease development in MRL/lpr mice. *Am. J. Pathol.* **161**, 1077–1086 (2002).
59. Miwa, T. et al. Decay-accelerating factor ameliorates systemic autoimmune disease in MRL/lpr mice via both complement-dependent and -independent mechanisms. *Am. J. Pathol.* **170**, 1258–1266 (2007).
60. Cossarizza, A. et al. Guidelines for the use of flow cytometry and cell sorting in immunological studies (second edition). *Eur. J. Immunol.* **49**, 1457–1973 (2019).

Acknowledgements

We would like to thank the excellent contributions from the iMM flow cytometry, rodent, and microscopy facilities. The project that gave rise to these results has received funding from the following sources:"la Caixa" Foundation under the grant agreement LCF/PR/HR19/52160005; European Union's Horizon 2020 Research and Innovation Programme under grant agreements No 667824; FCT - Portuguese Foundation for Science and Technology under grant agreements (PD/BD/138847/2018) (COVID/BD/152538/2022) (L.B.) SFRH/BD/131605/2017 (P.F-C), COMPETE LISBOA-01-0145-FEDER-028003, and 2021.01136.CEECIND (C.F), FCT - Fundação para a Ciência e a Tecnologia, I.P., under the project LA/P/0082/2020, for work in the Veldhoen laboratory: and FCT PD/BD/135481/2018 (D.P.), UIDB/04612/2020, UIDP/04612/2020 and LA/P/0087/2020 for work in the Silva Pereira laboratory; FCG - Fundação Calouste Gulbenkian within the Post-Graduation Programme for Science and Development (N.S.), FCT CEECIND/02373/2020 and FCG, FCT and "la Caixa" Foundation under the grant agreement HR22-00722 for work in the Amorim laboratory. The authors wish to acknowledge Brian Chan and Pedro Papotto, Lydia Becker Institute for Immunology & Inflammation, Faculty of Biology, Medicine & Health, Manchester Academic Health Science Centre, University of Manchester, United Kingdom for the delivery of *N. brasiliensis*.

Author contributions

L.B., C.F. performed the experiments and analysis, with additional technical help from P.F.-C., S.A., J.F., S.R., M.B., and S.A. Aspergillus were grown and quality checked by D.P. and C.S.P. Influenza virus stocks and technical help from N.S. and M.J.A. C.F. and M.V. conceived and design the project. C.F., M.J.A., C.S.P., and M.V. supervised the work. All authors contributed to the data discussion and the writing of the manuscript.

Competing interests

The authors declare no competing interests.

Additional information

Supplementary information The online version contains supplementary material available at https://doi.org/10.1038/s41467-023-41364-w.

Correspondence and requests for materials should be addressed to Marc Veldhoen or Cristina Ferreira.

Peer review information *Nature Communications* thanks Lalit Beura and the other, anonymous, reviewer(s) for their contribution to the peer review of this work.